Enhancement in the Gas Permeabilities of Novel Polysulfones with Pendant 4-Trimethylsilyl-α-hydroxylbenzyl Substituents†

Ying Dai,‡ Michael D. Guiver,*,‡ Gilles P. Robertson,‡ Yong Soo Kang,§ and Kwi Jong Lee||

National Research Council of Canada, Institute for Chemical Process and Environmental Technology, Ottawa, Ontario, K1A 0R6, Canada, Korea Institute of Science and Technology, Center for Facilitated Transport Membranes and Polymer Physics Lab, P.O. Box 131, Cheongryang, Seoul 130-650, Korea, and Seoul National University, Hyperstructured Organic Materials Research Center and School of Chemical Engineering, Seoul 151-744, Korea

Received May 15, 2003; Revised Manuscript Received June 25, 2003

ABSTRACT: A series of modified polymers with 4-trimethylsilyl-α-hydroxylbenzyl (HBTMS) substituents were made as new materials for membrane gas separation. HBTMS was introduced onto polysulfone (PSf), tetramethylpolysulfone (TMPSf), and hexafluoropolysulfone (6FPSf) by forming lithiated polymer intermediates followed by treatment with an electrophile, *p*-trimethylsilylbenzaldehyde. The resulting side substituent contains the bulky trimethylsilyl (TMS) groups separated from the polymer chain by an aromatic ring. The polymer structures were characterized by NMR spectroscopy, and thermal properties were investigated by differential scanning calorimetry and thermogravimetry. The permeability coefficients of the resulting polymers PSf-HBTMS, TMPSf-HBTMS, and 6FPSf-HBTMS showed considerable increases over the unmodified polymers. TMPSf-HBTMS showed the greatest improvements in gas transport properties with large increases in both CO_2 and O_2 permeabilities of ∼3-fold (72 and 18 Barrers, respectively) compared with TMPSf. In the case of the CO_2/N_2 gas pair, there was an absence of the typical accompanying tradeoff shown by decreases in permselectivity with increasing permeability. Comparisons of this series of polymers containing the new HBTMS substituent were made with those having other TMS pendant groups.

Introduction

The separation of gases by synthetic membranes is a dynamic and rapidly growing field. Membrane separation processes offer a number of advantages over traditional methods in terms of capital investments and lower energy use.[1] Polysulfone (PSf) has adequate gas separation performance[2−4] as well as good thermostability, mechanical properties, and chemical resistance. It was the first commercial polymer used for fabricating gas separation membranes in the form of hollow fibers for the separation of H_2 and the production of N_2 because of its overall combination of adequate gas permeabilities and relatively high permselectivities to various gas pairs as well as its good mechanical properties for fiber spinning.[5] The previous work most relevant to the present work was by Koros and Paul whereby parallel families of polysulfones with systematic structural modifications were correlated with their gas separation properties.[6−10]

Both tetramethylpolysulfone (TMPSf) and hexafluoropolysulfone (6FPSf) are more permeable than PSf but maintain comparable permselectivity for many gas pairs[9,10] because tetramethyl and hexafluoroisopropylidene groups sterically hinder both bond rotation and intersegmental packing. The packing of 6FPSf may be further inhibited by intermolecular repulsive forces between fluorine atoms that have high electron density.[9] It is known that trimethylsilyl (TMS) groups in the polymer backbone enhance polymer solubility without significant loss of thermal stability. In addition, they hinder chain motions and disrupt chain packing thereby improving gas permeability with minimal loss in permselectivity.[11−17]

The chemical structure and physical properties of the membrane material influence the permeability and permselectivity.[18] Transport properties depend on the free volume within the polymer and on the segmental mobility of the polymer chains. The segmental mobility of the polymer chains is affected by factors such as the extent of unsaturation, degree of cross-linking, degree of crystallinity, and nature of substituent. The glass transition temperature (T_g) of polymers has a profound influence on transport properties. For the majority of polymers, those with lower T_g values possess greater segmental mobilities, which result in higher diffusivities.[19] Many studies have shown that an improvement in gas transport properties could be obtained by modifying or tailoring the polymer structure. Polarity and steric characteristics of the polymeric material strongly influence gas permeation. The size and shape of bulky groups placed on the polymer chain affect certain fundamental properties such as packing density and rigidity. The substitution of bulky groups in the side chains appears to have a greater influence on diffusivity than substitution of these groups in the polymer backbone. An absence of such groups tends to increase the structural regularity and increases density.[1,19]

Chemical modification of PSf's was performed in order to improve membrane separation properties. PSf's were activated by direct lithiation[20] or by bromination−lithiation[21] to produce reactive lithiated intermediates that were then converted by various electrophiles to

* Corresponding author. Address: National Research Council, Institute for Chemical Process and Environmental Technology, 1200 Montreal Road, Ottawa, Ontario, K1A 0R6, Canada. E-mail: michael.guiver@nrc-cnrc.gc.ca.

† NRCC No. 46443.

‡ National Research Council of Canada.

§ Korea Institute of Science and Technology.

|| Seoul National University.

10.1021/ma0346411 CCC: $25.00
Published on Web 08/12/2003

yield derivatives of PSf.[11,12,22−26] In comparison with previous work in which TMS, dimethylphenylsilyl (DMPS), and methyldiphenylsilyl (MDPS) groups were introduced on PSf and TMPSf,[11,12,26] this work reports the improvements in gas permeability for polymers PSf, TMPSf, and 6FPSf modified to contain the new bulky side substituent 4-trimethylsilyl-α-hydroxylbenzyl (HBTMS). HBTMS contains TMS, phenyl, and OH groups and is distinct from TMS and DMPS since the TMS group is spaced further from the polymer chain. The phenyl spacer and hydroxyl group may contribute to increase the rigidity because of changing structural regularity and H-bonding. Another polymer, PSf-CH_2-TMS, was prepared containing a flexible $-CH_2-$ spacer between polymer and TMS. In comparison with polymers containing the rigid HBTMS groups, this polymer had inferior gas transport properties.

Experimental Section

Materials. Monomers hexafluorobisphenol A (Aldrich Chemical Co.) and 4,4′-dichlorodiphenyl sulfone (Pfaltz & Bauer, Inc.) were further purified by crystallization from ethanol 95%. Before polymerization, all monomers were dried in a vacuum oven at 55 °C for 24 h. Anhydrous potassium carbonate (analytical reagent from BDH) was dried in an oven at 110 °C for 24 h. *N*-Methylpyrrolidinone (NMP) was distilled over barium oxide under a vacuum, and analytical reagent toluene from BDH was used as received. PSf-Br_2,[21] TMPSf-Br_2[12] and 6FPSf[8,9] were made following previously reported synthetic procedures. PSf Udel P-3500 (BP-Amoco), PSf-Br_2, TMPSf-Br_2, and 6FPSf were dried at 110 °C for at least 24 h before reaction. Reagent grade tetrahydrofuran (THF) was freshly distilled over lithium aluminum hydride ($LiAlH_4$). *n*-Butyllithium (10 M in hexane), bromine, 1-bromo-4-(trimethylsilyl)-benzene (BTMSB), (iodomethyl)trimethylsilane, and *N*,*N*-dimethylformamide (DMF) were obtained from Aldrich Chemical Co., and DMF was purified by azeotropic distillation with benzene (10% v/v, previously dried over CaH_2) before the reaction. Modification reactions were conducted under a constant argon purge and with mechanical stirring. A mixture of dry ice and ethanol was used for cooling reaction mixtures. All modified polymers were recovered by precipitation from ethanol using a Waring blender, washed thoroughly, and then dried in a vacuum oven at 55 °C.

Synthesis of *p*-Trimethylsilylbenzaldehyde (TMSBA). A solution of colorless liquid BTMSB (38.50 g, 168 mmol) in anhydrous THF (10 wt %) was cooled to −76 °C under argon, and 10 M *n*-butyllithium (17.7 mL, 177 mmol) was injected dropwise by syringe pump over 15 min. The reaction solution remained colorless. Following addition, the reaction mixture was stirred for 15 min to give a soluble lithiated intermediate; then excess purified DMF (30.7 g, 32.4 mL, 420 mmol) was added quickly into the reaction solution. When the solution was warmed gradually to −30 °C over about 1 h, 300 mL of saturated NH_4Cl solution and 100 mL of ethyl ether were added to the resulting colorless solution. The solution was shaken well, and the organic phase was separated and then washed with saturated NaCl solution, dried with anhydrous Mg_2SO_4, and evaporated to remove solvents. The product was purified by distillation under a vacuum to yield 26.76 g (89%) of TMSBA as a colorless oil. The resulting product was characterized by ^1H NMR ($CDCl_3$): CHO, 10.01 ppm, 1H, s; H-2, 7.83 ppm, 2H, dd ($^3J = 8$ Hz, $^4J = 2$ Hz); H-3, 7.68 ppm, 2H, dd ($^3J = 8$ Hz, $^4J = 2$ Hz); CH_3, 0.30 ppm, 9H, s.

Synthesis of PSf-*s*-HBTMS. A solution of PSf (15.0 g, 33.9 mmol) in anhydrous THF (1.7 wt %) was cooled to −73 °C using a dry ice/alcohol bath under argon, and 10 M *n*-butyllithium (7.46 mL, 74.6 mmol) was injected dropwise by syringe pump over 15 min during which time color changes were observed.[20,22,23] Following addition, the lithiated polysulfone solution was stirred for 15 min and then warmed gradually to −30 °C over about 1 h. TMSBA (16.3 g, 91.8 mmol) was injected promptly into the reaction solution, which immediately became cloudy white, and then the solution was stirred with gradual warming to −15 °C. The polymer was recovered by precipitation from ice water, washed with ice-ethanol, and dried in an oven at 110 °C. The white product (22.0 g) had a degree of substitution (DS) of 1.5.

Synthesis of PSf-*o*-HBTMS. A solution of PSf-Br_2 (5.0 g, 8.33 mmol) in anhydrous THF (1.7 wt %) was cooled to −73 °C under argon, and 2.5 M *n*-butyllithium (7.2 mL, 17.9 mmol) was injected dropwise by syringe pump over 15 min.[21] Following addition, the lithiated polymer solution was stirred for 15 min and then warmed to −30 °C. TMSBA (4.45 g, 25 mmol) was injected promptly into the reaction solution, which immediately became cloudy white. The solution was stirred with gradual warming to −15 °C over about 1 h. The polymer was recovered by precipitation from ice water, washed with ice-ethanol, and dried in an oven at 110 °C. The white product (4.55 g) had a DS of 1.7.

Synthesis of PSf-*o*-CH_2-TMS. A solution of PSf-Br_2 (5.5 g, 9.16 mmol) in anhydrous THF (1.0 wt %) was lithiated with 10 M *n*-butyllithium (1.97 mL, 19.7 mmol) using the above procedure. (Iodomethyl)trimethylsilane (9.8 g, 6.8 mL, 45.8 mmol) was injected promptly into the −40 °C reaction solution, which immediately became cloudy white. The solution was stirred with gradual warming to −5 °C over about 1 h. The polymer was recovered by precipitation from 95% ethanol, washed with ethanol, and dried in an oven at 110 °C. The white product (4.59 g) had a DS of 1.1.

Synthesis of 6FPSf-Br_2. Excess bromine (45 mL, 139.5 g, 0.872 mol) was added to a magnetically stirred solution of 6FPSf[8,9] (15 g, 27.2 mmol) in chloroform (300 mL) at room temperature and under an argon atmosphere. The dark red homogeneous mixture was left stirring at room temperature for 16 h. The polymer was precipitated using methanol. The recovered polymer was left standing in fresh methanol to leach out residual free bromine and then filtered again and dried in a vacuum oven for 24 h at 55 °C. White 6FPSf-Br_2 polymer (19 g; yield, 98%) was recovered. Elemental Analysis: calcd for $C_{27}H_{14}Br_2O_4S$, 22.56% Br; found, 23.13% Br.

Synthesis of 6FPSf-*o*-HBTMS. A colorless solution of 6FPSf-Br_2 (5.25 g, 7.42 mmol) in anhydrous THF (1.3 wt %) was cooled to −76 °C under argon, and 10 M *n*-butyllithium (1.6 mL, 16.0 mmol) was injected dropwise by syringe pump over 15 min. Following addition, the clear orange solution was stirred for 15 min and then warmed to −36 °C over about 1 h. TMSBA (3.96 g, 22.3 mmol) was injected promptly into the reaction solution, which immediately became cloudy yellow-white. The solution was stirred with gradual warming to −15 °C. The polymer was recovered by precipitation from ice water, washed with ice-ethanol, and dried in an oven at 110 °C. The white product (3.98 g) had a DS of 1.7.

Synthesis of TMPSf-HBTMS. A cloudy yellow solution of TMPSf-Br_2[12] (5.03 g, 7.66 mmol) in anhydrous THF (1.0 wt %) was cooled to −77 °C under argon, and 10 M *n*-butyllithium (1.7 mL, 16.5 mmol) was injected dropwise by syringe pump over 15 min.[12] Following addition, the lithiated polymer solution was stirred for 15 min and then warmed to −30 °C. TMSBA (4.09 g, 23 mmol) was injected promptly into the reaction solution, which immediately became cloudy yellow-white. The solution was stirred with gradual warming to −15 °C over about 1 h. The polymer was recovered by precipitation from ice-ethanol, washed with ice-ethanol, and dried in an oven at 110 °C. The white product (3.98 g) had a DS of 1.5.

Characterization Methods. Nuclear magnetic resonance spectra were recorded on a Varian Unity Inova spectrometer at a resonance frequency of 399.961 MHz for ^1H and 100.579 MHz for ^{13}C. Samples were prepared using $CDCl_3$ as the NMR solvent, and the residual $CHCl_3$ signal at 7.25 ppm was used as the chemical shift reference. The inherent viscosities of polymers were determined using an Ubbelohde viscometer at a polymer concentration of 0.4 g/dL in NMP at 35 °C. The DS of modified polymers was readily determined using ^1H NMR by comparison of the integration values for selected signals (described later). Polymer thermal degradation curves were obtained from thermogravimetric analysis (TGA) (TA Instru-

Scheme 1. Synthesis of TMSBA

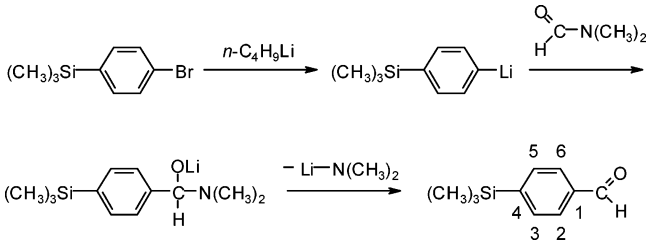

ments model 2950), and glass transition temperatures (T_g) were obtained from differential scanning calorimetry (DSC) (TA Instruments model 2920). Polymer samples for TGA were preheated to 60 °C for 2 h inside the TGA furnace for moisture removal under nitrogen gas and then heated to 600 °C at 10 °C/min for degradation temperature measurement. Samples for DSC were heated initially to at least 30 °C above T_g at 10 °C/min under a flow of 50 mL/min of nitrogen gas, quenched with liquid nitrogen, and reheated at 10 °C/min for the T_g measurement.

X-ray diffraction was used to investigate *d*-spacing. A Macscience model M18XHF22 was utilized with Cu Kα radiation of which the wavelength (λ) was 1.54 Å at 50 kV and 100 mA and the scanning speed was 5°/min. The value of the *d*-spacing was calculated by means of Bragg's law ($d = \lambda/2 \sin \theta$), using θ of the broad peak maximum.

Dense polymer films for permeability measurements were made from 5 wt % polymer solutions in anhydrous THF that were filtered through 1 μm poly(tetrafluoroethylene) filters and then poured into flat-glass dishes and dried under a nitrogen atmosphere at room temperature. The detached films were further dried for 3 days in a vacuum oven at 40 °C to remove the residual solvent. Optically clear films were obtained with a thickness of about 40 μm in all cases. The absence of residual solvent in the films was confirmed by observing T_g using DSC. Permeability coefficients of carbon dioxide, oxygen, and nitrogen were measured by the constant volume method at 35 °C with an upstream pressure of 1 atm.

Results and Discussion

Preparation of Polymers. Aldehyde is strongly reactive toward carbanions and other nucleophiles. TMSBA was prepared as a reactive electrophile to introduce HBTMS substituents onto PSf, TMPSf, and 6FPSf using a lithiation reaction. TMSBA was prepared by lithium−bromine exchange followed by treatment with DMF as shown in Scheme 1. The low reaction temperature was necessary to obtain higher product yield. This is an alternative and convenient method for the synthesis of aromatic aldehydes that are often prepared by oxidation of methylbenzenes or reduction of acid chlorides.

The synthetic route for the preparation of PSf-*s*-HBTMS by direct lithiation is shown in Scheme 2. The procedures for the synthesis of the other polymers PSf-*o*-HBTMS, PSf-*o*-CH_2-TMS, 6FPSf-*o*-HBTMS, and TMPSf-HBTMS are all based on bromination−lithiation. Brominated polymers PSf-Br_2[21] and TMPSf-Br_2[12] were prepared as previously reported. 6FPSf-Br_2 was prepared by the addition of excess bromine to a 6FPSf polymer solution in $CHCl_3$. The reactive substitution position is situated ortho to the aryl ether linkage in the bisphenol portion of the repeat units as shown in Scheme 3. This is the most favorable site because it is electrophilically activated by the oxygen atom. The variation in reaction times for preparing TMPSf-Br_2 (1 h), PSf-Br_2 (6 h), and 6FPSf-Br_2 (16 h) for DS = 2 was because of the different electrophilic reactivities. TMPSf is the most electrophilically activated toward bromination in the reactive position because of four methyl groups, whereas 6FPSf is deactivated because of the electron-withdrawing effect of the two $-CF_3$ groups.

Scheme 2. Synthesis of PSf-*s*-HBTMS

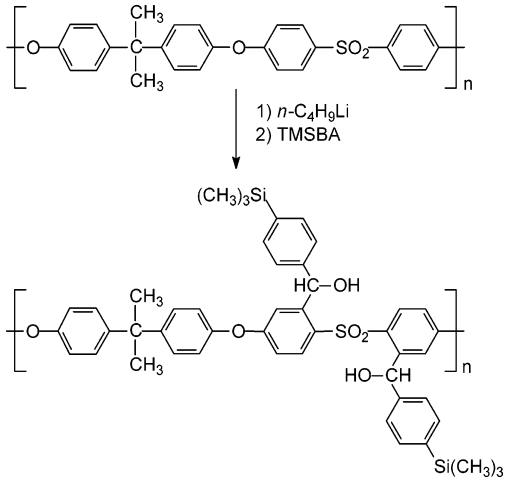

Scheme 3. Synthesis of 6FPSf-*o*-HBTMS

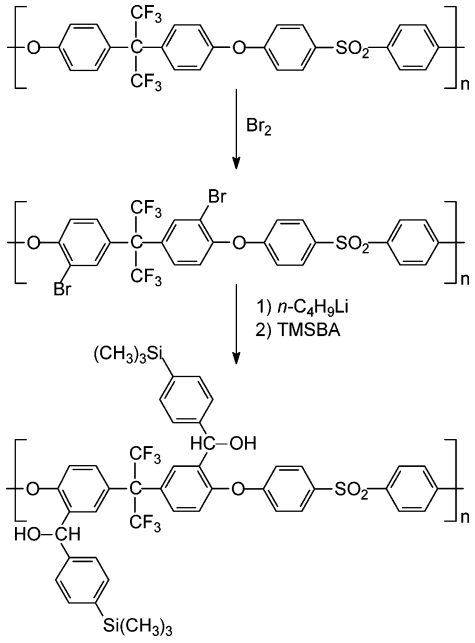

The brominated polymers were first reacted with 2.1 mol equiv of *n*-butyllithium respectively in order to exchange bromine for lithium, followed by reaction with the electrophile TMSBA or (iodomethyl)trimethylsilane. The synthetic routes are given in Schemes 2−6, and the DSs of the polymers PSf-*s*-HBTMS, 6FPSf-*o*-HBTMS, PSf-*o*-HBTMS, PSf-*o*-CH_2-TMS, and TMPSf-HBTMS were 1.5, 1.7, 1.7, 1.1, and 1.5, respectively, determined by NMR. PSf-*s*-HBTMS had a lower DS than PSf-*o*-HBTMS because of HBTMS substituent steric hindrance around the diphenyl sulfone segment. PSf-*o*-CH_2-TMS had a low DS compared with PSf-*o*-HBTMS because (iodomethyl)trimethylsilane has lower reactivity than TMSBA. TMPSf-HBTMS had a lower DS because of steric hindrance from $-CH_3$, preventing complete access of HBTMS substituents.

Structural Characterization (NMR). The ^1H NMR spectra of PSf and 6FPSf derivatives with substituted TMSBA are shown in Figures 1 and 2. The ^1H NMR chemical shift displacements (ppm) and multiplicity data (s, singlet; d, doublet; m, multiplet) of aromatic and

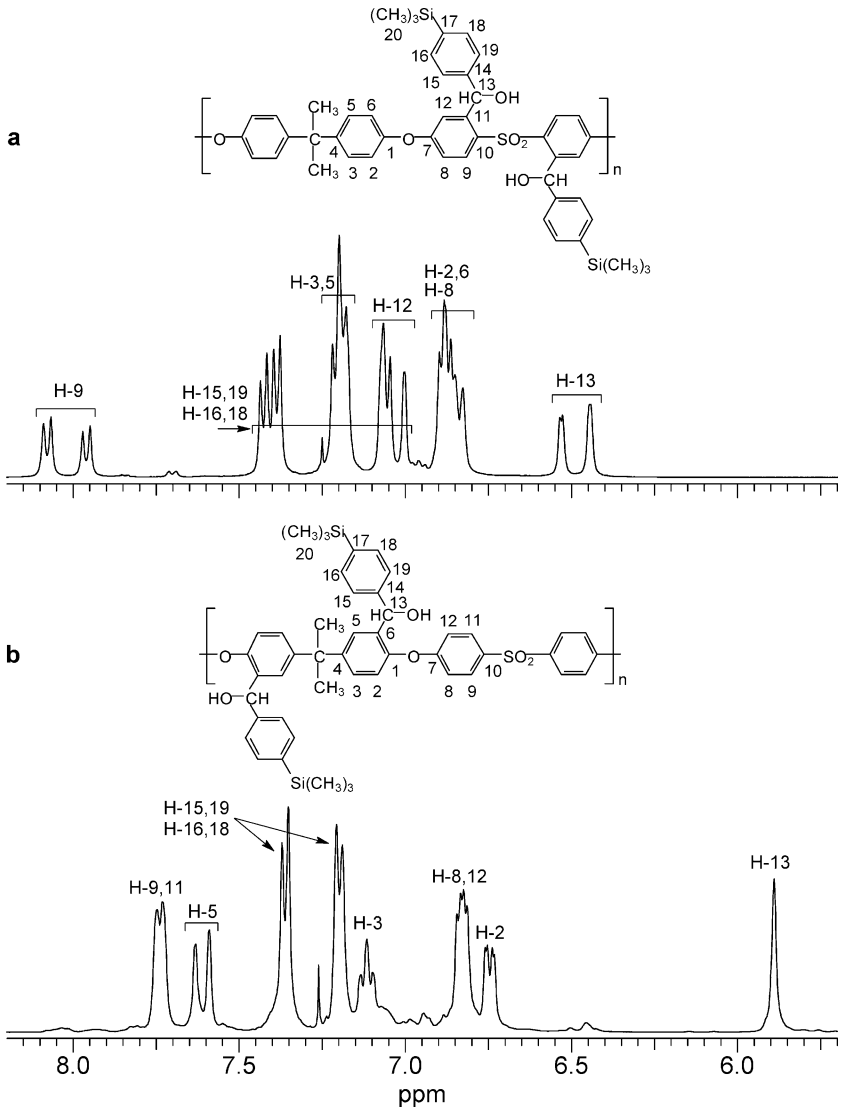

Figure 1. ^{1}H NMR spectra of PSf-*s*-HBTMS and PSf-*o*-HBTMS.

aliphatic signals are listed in Tables 1 and 2. The spectra show expansions of the aromatic regions where the results of the substitution reaction can be observed from the changing NMR signals. Evidence of the successful incorporation of HBTMS groups on the main polymer chain was also evident at high field where the TMS signal could be observed (Tables 1 and 2).

The NMR spectra of the aromatic regions of PSf substituted at the ortho-sulfone and ortho-ether linkage sites (Schemes 2 and 3) are displayed in parts a and b of Figure 1, respectively. The high DSs obtained for each of these derivatives (PSf-*s*-HBTMS DS = 1.5, PSf-*o*-HBTMS DS = 1.7) resulted in simplified spectra due to signals originating primarily from disubstituted repeat units. On the other hand, the bulkiness of the substituents had a significant effect on polymer chain protons nearest to the substituents. This was especially apparent in the ortho-sulfone derivative where both substituents are localized around the sulfone linkage. This hinders rotation about the aryl−sulfone−aryl bonds, resulting in multiple signals for the same protons. Moreover, possible hydrogen bonding between the −OH groups could be another factor impacting rotational mobility. As a result, most proton signals from HBTMS substituents (H-13, 15, 16, 18, 19, −OH) as well as from the main chain aryl groups around the sulfone functionality (H-8, 9, 12) each appear as two signals rather than one signal; this is particularly obvious in the case of H-9 and H-13 (Figure 1a). On the other hand, the ortho-ether linkage substituted polymer (Figure 1b) displays a much simpler spectrum where only the hydrogen atoms of the polymer chain aryl groups bearing the substituents appear as multiplets. Aryl protons H-2, H-3 and H-8, H-12 are slightly split by steric hindrance due to the substituents, while H-5 is clearly more affected (two resolved signals) because of its close proximity with HBTMS. The presence of an asymmetric carbon (H−C*−OH) should not play a significant role in this observed spitting of the signals since the mixture of isomers is expected to be exactly 1:1 for this type of reaction on an aldehyde electrophile. The chemical shift of H-13 on the asymmetric carbon was observed to be dependent upon the site of substitution (ortho sulfone or ether). Differences in electron shielding around H-13 due to its orientation in space vary for each derivative. The distinct upfield signal for H-13 was split into two for the ortho-sulfone HBTMS substituted polymer, while the ortho-ether derivative led to a singlet for the same H-13. This emphasizes what was described earlier as restricted mobility of substit-

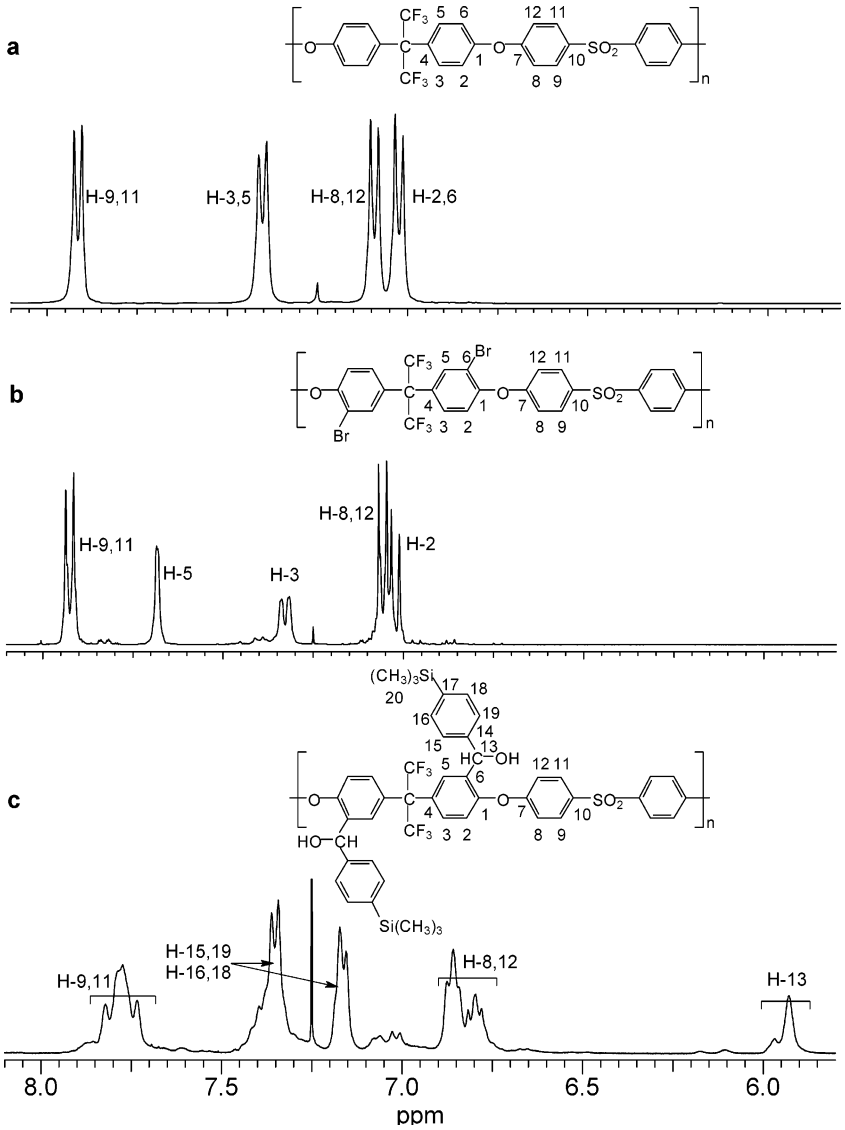

Figure 2. ^{1}H NMR spectra of 6FPSf and selected derivatives.

uents near the sulfone linkage. Furthermore, the protons of the substituent aryl groups also display the same behavior as seen for H-13: a multiple signal in the ortho-sulfone polymer compared with two coupled doublets for H-15, 19 and H-16, 18 for the ortho-ether polymer. The −OH signals for both modified polymers appear at high field around 3 ppm.

The ^{1}H NMR chemical shift displacements (ppm) of PSf-Br_2 modified with (iodomethyl)trimethylsilane (Scheme 4) are listed in Table 1. Once again, the high-field trimethylsilyl signals (−0.19−0.21 ppm) as well as the new CH_2 singlet at 1.88 ppm are an indication of the presence of the new substituent.

TMSBA was also substituted on 6FPSf-Br_2 (Scheme 5). The ^{1}H NMR spectrum of 6FPSf-Br_2 (Figure 2b) consists of the expected two spin systems: one involving H-8, 12 with H-9, 11 and another system involving H-3 with H-2 and H-5. The spectrum of ortho-ether substituted 6FPSf-Br_2 (Figure 2c) with TMSBA resembles that of the PSf analogue (Figure 1b). The DS was 1.7, hence the presence of mostly disubstituted repeat units. However, the ^{1}H NMR spectrum was more complicated because it had more overlapping signals than previous spectra; H-2, 3, and 5 could not be assigned. In contrast, the presence of the HBTMS substituents at the ortho-ether sites was easily confirmed by signals at similar chemical shifts as seen before in Figure 1b. The two spin-coupled doublets H-15, 19 and H-16, 18 as well as the singlet H-13 at high field (6 ppm) and the −OH signal (3 ppm) were the proof of HBTMS substitution.

The full ^{1}H NMR spectrum and NMR data of the HBTMS substituted polymer TMPSf-Br_2 (Scheme 6) are displayed in Table 3 and Figure 3. Although the spectrum appears complicated, it was found that substitution occurred at both the ortho-sulfone and ortho-ether sites as observed previously,[12] due to nonregioselectivity of the lithiation reaction for this particularly hindered polymer. The complex NMR spectrum is a result of a mixture of many different repeat units.

The DS of all previously described modified polymers was assessed by comparative integration of specific NMR signals. One method consisted of comparing either the intensity of the distinct H-13 signal or that of the high-field TMS methyl groups with that of the six isopropylidene protons of PSf. Another method derived from ref 27 required the integration values of the signals at low field exclusively. This method was utilized and was particularly useful for measuring the DS of substituted 6FPSf.

Table 1. ^{1}H NMR Data for PSf and Selected Derivatives

proton number	PSf	PSf-*s*-HBTMS	PSf-*o*-HBTMS	PSf-*o*-CH_2-TMS
H2	6.93 (d, *J* 8.8)	6.78−6.93 (m)	6.73 (d, *J* 8.4) 6.74 (d, *J* 8.4)	6.80 (d, *J* 8.4)
H3	7.24 (d, *J* 8.8)	7.13−7.26 (m)	7.11 (dd, *J* 8.4, 2.3) 7.09 (dd, *J* 8.4, 2.3)	6.88 (dd, *J* 8.4, 2.2)
H5	7.24 (d, *J* 8.8)	7.13−7.26 (m)	7.62 (d, *J* 2.4) 7.58 (d, *J* 2.4)	6.91−7.40 (m)
H6	6.93 (d, *J* 8.8)	6.78−6.93 (m)		
H-3′,5′				7.24 (d, *J* 8.8)
H-2′,6′				7.01 (d, *J* 8.8)
H8	7.00 (d, *J* 8.8)	6.78−6.93 (m)	6.78−6.86 (m)	6.91−6.97 (m)
H9	7.84 (d, *J* 8.8)	8.07 (d, *J* 8.8) 7.95 (d, *J* 8.8)	7.68−7.77 (m)	7.80−7.88 (m)
H11	7.84 (d, *J* 8.8)		6.78−6.86 (m)	7.80−7.88 (m)
H12	7.00 (d, *J* 8.8)	6.98−7.09 (m)	6.78−6.86 (m)	6.91−6.97 (m)
H13		6.53 (d, *J* 4.0) 6.44 (d, *J* 3.0)	5.88 (s)	1.88 (s)
H-15, 16, 18, 19		7.42 (d, *J* 8.0) 7.38 (d, *J* 8.0) 7.13−7.26 (m) 6.98−7.09 (m)	7.35 (d, *J* 7.5) 7.19 (d, *J* 7.5)	
O*H*		3.44 (s) 3.01 (s)	2.3−2.7 (broad)	
H-20 (SiCH_3)		0.24 (s)	0.19 (s)	−0.19−0.21 (m)
CH_3−C−CH_3	1.69 (s)	1.67 (s)	1.71 (s)	1.60−1.75 (m)

Table 2. ^{1}H NMR Data 6FPSf and Selected Derivative

proton number	6FPSf	6FPSf-Br_2	6FPSf-HBTMS
H2	7.02 (d, *J* 8.8)	7.02 (d, *J* 8.8)	6.7−8.0
H3	7.41 (d, *J* 8.8)	7.33 (dd, *J* 8.8, 2.4)	6.7−8.0
H5	7.41 (d, *J* 8.8)	7.69 (d, *J* 2.4)	6.7−8.0
H6	7.02 (d, *J* 8.8)		
H8-12	7.09 (d, *J* 8.8)	7.06 (d, *J* 8.8)	6.75−6.90 (m)
H9-11	7.92 (d, *J* 8.8)	7.93 (d, *J* 8.8)	7.70−7.90 (m)
H13			5.93 (s) 5.97 (s)
H15, 16, 18, 19			7.13−7.20 (m) 7.30−7.40 (m)

Scheme 4. Synthesis of PSf-*o*-HBTMS

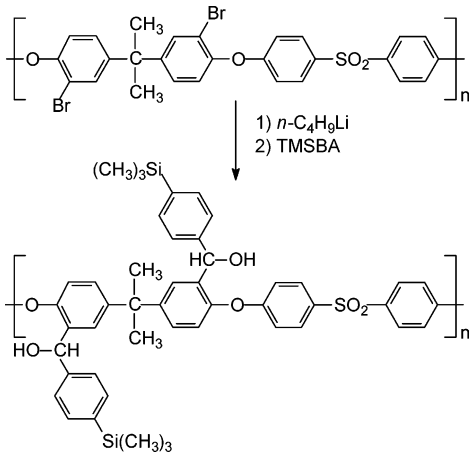

$$\frac{H_{13}}{H_a} = \frac{n}{16 - n + 4n}$$

hence

$$n = \frac{16H_{13}}{(H_a - 3)H_{13}} \quad \text{for PSf and 6FPSf}$$

where H_{13} is the intensity of the H-13 signal, H_a is the total intensity of aromatic signals, and n is the degree of substitution (0−2).

Scheme 5. Synthesis of PSf-*o*-CH_2-TMS

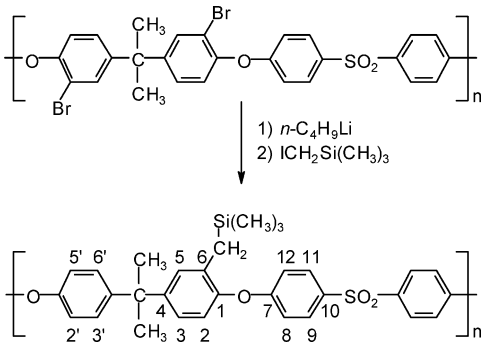

Scheme 6. Synthesis of TMPSf-HBTMS

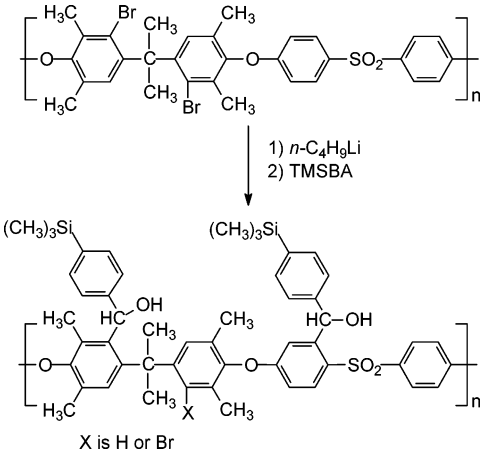

Solubility Test. Solubility was observed during the day of sample preparation and then 14 days later to determine if the solutions were stable. All the polymers dissolved in $CHCl_3$.

Thermal Measurements. The thermal stabilities of PSf derivatives were measured by TGA, and the weight-loss data are shown in Table 4. All derivative polymers were thermally less stable than the respective parent polymers. The curves of all the polymers exhibited a two-step degradation. This suggests that during the

Table 3. ^{1}H NMR Data for TMPSf and Selected Derivatives

proton number	TMPSf	TMPSf-Br_2	TMPSf-HBTMS
H3	6.94 (s)	7.44 (s)	6.6−8.3
H3′			6.6−8.3
H5	6.94 (s)		6.6−8.3
H8	6.83 (d, *J* 8.8)	6.83 (d, *J* 9.2)	6.6−8.3
H9	7.81 (d, *J* 8.8)	7.84 (d, *J* 8.8)	6.6−8.3
H11	7.81 (d, *J* 8.8)	7.84 (d, *J* 8.8)	6.6−8.3
H12	6.83 (d, *J* 8.8)	6.83 (d, *J* 9.2)	6.6−8.3
H-13			5.7−6.5 (m)
O*H*			2.5−3.4 (m)
H15, 16, 18, 19			6.6−8.3
H-20 (SiCH_3)			0.18−0.26 (m)
ArCH_3	2.03 (s)	C2−CH_3 2.09 (s) C6−CH_3 2.11 (s)	1.4−2.2 (m)
CH_3−C−CH_3	1.69 (s)	1.67 (s)	1.4−2.2 (m)

Table 4. Glass Transition Temperatures (T_g's) and Thermal Degradation of Polymers

polymer	DS	T_g, °C	actual onset, °C	extrapolated onset, °C
PSf		188.1	455.0	521.1
PSf-Br_2	2.0	191.0	287.6	430.4
PSf-*s*-HBTMS	1.5	179.7	304.4	303.1
PSf-*o*-HBTMS	1.7	166.2	319.8	335.7
PSf-*o*-CH_2-TMS	1.1	142.7	339.4	393.7
6FPSf		199.4	486.8	514.0
6FPSf-Br_2	2.0	196.4	465.2	505.2
6FPSf-*o*-HBTMS	1.7	186.5	343.4	358.9
TMPSf		231.3	396.0	432.1
TMPSf-Br_2	2.0	275.4	310.0	425.2
TMPSf-HBTMS	1.5	230.3	312.2	320.7

heating process, HBTMS was lost from polymer first. For example, the extrapolated onsets of weight loss for PSf-*o*-HBTMS occurred at 353.7 °C and the actual onsets of degradation occurred at 321.2 °C. The initial-step degradation of PSf-*o*-HBTMS is believed to be the loss of $-Si(CH_3)_3$ since the weight loss is close to the theoretical weight loss of 17% from PSf-*o*-HBTMS with DS = 1.7. The second degradation for PSf-*o*-HBTMS is believed to be the loss of the entire substitution group since the weight loss is close to the theoretical weight loss of 40% from PSf-*o*-HBTMS with DS = 1.7. These data are in agreement with the DS results from NMR. A possible explanation for the lower thermal stability of the ortho-sulfone derivatives could be a combination of steric hindrance about the diphenyl sulfone site and a bulky side group as well as the strong electron-withdrawing ability of the sulfone group, resulting in a weakening of the carbon−silicon bond.[11,17]

All PSf polymer derivatives had lower T_g values than PSf. PSf-*s*-HBTMS had a T_g ~13 °C higher than that of PSf-*o*-HBTMS. PSf-*o*-CH_2-TMS had a very low T_g of 142.7 °C most likely because of the relatively greater mobility of the alkyl spacer compared with the HBTMS substituent. 6FPSf-*o*-HBTMS showed a T_g reduction of 10 °C compared with 6FPSf. This was possibly due to a loss in symmetry of the phenylene ring by the introduction of HBTMS. The T_g of TMPSf-HBTMS was approximately the same as TMPSf. This suggests the HBTMS increased the chain stiffness while reducing the intermolecular interactions.

Gas Transport Properties. A tradeoff relationship is usually observed between permeability (P) and permselectivity (α) for common gases in glassy or rubbery polymers. That is, higher permeability is gained at the cost of lower permselectivity and vice versa. Upper bound performance lines for the relationship between gas permeability and permselectivity have been proposed by Robeson et al.[3] A new calculation method to show the distance (δ) from the permeability point (P_i, vs α_{ij}, where permselectivity $\alpha_{ij} = P_i/P_j$) to the upper bound line[3] was developed in this work. This gives a quantitative and convenient measure of the overall improvement in permeability/permselectivity that occurs from a polymer modification. The following equation was used to calculate the upper bound line according to Robeson's work:[3]

$$P_i = k_1 \alpha_{ij}^{n_1} \tag{1}$$

$$\log \alpha_{ij} = -n \log P_i + \log k \tag{2}$$

where $n = d_j - d_i$ where d_j is the kinetic diameter of the lower permeability gas and d_i is the kinetic diameter of the higher permeability gas. The kinetic diameters as reported by Breck[28] are listed in Table 5. The exact position of the upper bound line was chosen from the best data of Park et al.[2] For the O_2/N_2 gas pair, poly(tetrabromofluorene tetrabutyl isophthalate) gives the

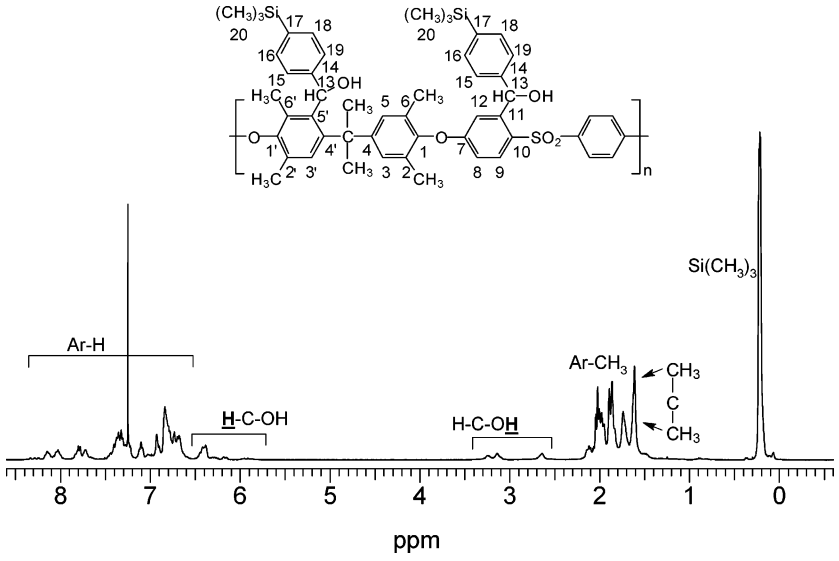

Figure 3. ^{1}H NMR spectra of TMPSf-HBTMS.

Table 5. Lennard-Jones Kinetic Diameters of Various Gases[a]

	gas					
	He	H_2	CO_2	O_2	N_2	CH_4
kinetic diameter (Å)	2.6	2.89	3.3	3.46	3.64	3.8

[a] Reference 28.

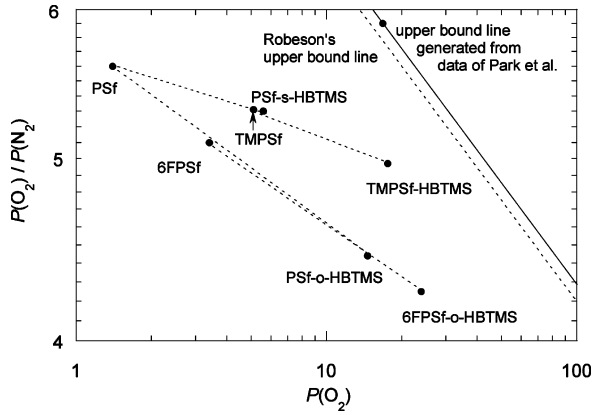

Figure 4. Gas permeabilities of modified PSf's for O_2 and N_2 in relation to the upper bound line of Robeson (ref 3) (dashed line) and one generated from data in Park et al. (ref 2) (solid line).

best data ($P(O_2) = 16.8$, $\alpha(O_2/N_2) = 5.9$) and was selected as the point from which to draw the upper bound line according to eq 2. If instead Robeson's data[3] were to be selected, the distance to the upper bound (δ) would be shorter by $\sim 15 \times 10^{-3}$ for the O_2/N_2 gas pair and $\sim 5 \times 10^{-3}$ for the CO_2/N_2 gas pair. Using the data of Park et al.[2] and $n = d_{N_2} - d_{O_2} = 3.64 - 3.46 = 0.18$, a value of k in eq 2 can be calculated. Therefore the upper bound line equation can be obtained. Using a mathematical method, the distance from a permeability/permselectivity point to the upper bound line can be calculated according to eq 3.

$$\delta = (\log k - \log \alpha_{ij} - n \log P_i) \cos(\arctan(n)) \quad (3)$$

Single gas permeability coefficients (P) were measured on polymer dense films for CO_2, O_2, and N_2 using the constant downstream volume method. A summary of d-spacing, permeability coefficients, and permselectivities for these gases and the δ values are summarized in Table 6, and the gas permeation improvement trends are shown in Figures 4 and 5. The distances in Table 6 are to the upper bound lines that were generated from the data of Park et al.[2] In both Figures 4 and 5, the

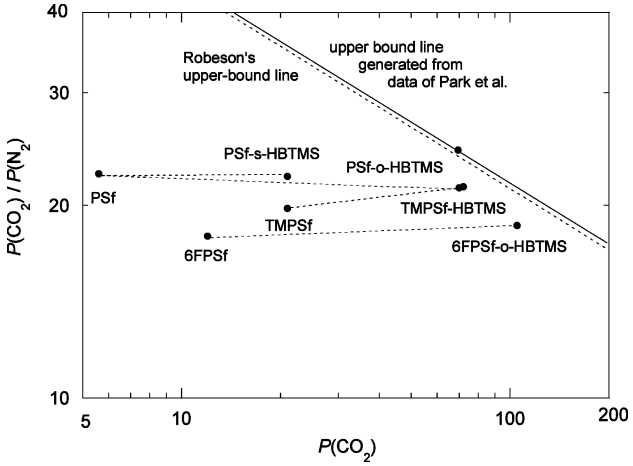

Figure 5. Gas permeabilities of modified PSf's for CO_2 and N_2.

dashed lines represent the Robeson upper bound lines whereas the solid lines represent the generated upper bound lines from the data of Park et al.[3] Each point on the upper bound lines in Figures 4 and 5 refers to poly(tetrabromofluorene tetrabutyl isophthalate), the reference polymer giving the best data from Park et al. for both O_2/N_2 and CO_2/N_2 gas pairs.

All the polymers containing the HBTMS substituent were significantly more permeable to all gases than their parent polymers PSf, 6FPSf, and TMPSf. What is notable is the small or absent decrease in permselectivity, particularly for the CO_2/N_2 gas pair. The HBTMS substituent has a TMS group spaced from the polymer chain by a rigid phenyl and H-bonded hydroxyl groups. The open structure leads to high gas permeability, while the rigid substituent provides a selective diffusion environment.

In comparison with PSf, PSf-*o*-HBTMS showed large increases in CO_2 and O_2 permeability (~13-fold and 10-fold) with a simultaneously lesser reduction in permselectivity as measured by a lessening of distances δ to the upper bound line (from 0.387 to 0.054 and from 0.213 to 0.133, respectively) and the d-spacing increased from 5.0 to 5.3 Å. As shown in Table 6 and Figures 4 and 5, the gas transport data for PSf-*s*-HBTMS and PSf-*o*-HBTMS were better than those of PSf. The substitution site for the HBTMS group is important especially in terms of the extent of permeability increase since the data for PSf-*o*-HBTMS were better than those of PSf-

Table 6. Gas Permeabilities of Modified PSf's

		P, Barrer[a]			α[b]		$\delta \times 10^3$	
polymer	d-spacing	CO_2	O_2	N_2	CO_2/N_2	O_2/N_2	CO_2/N_2	O_2/N_2
PSf	5.0	5.6	1.4	0.25	22.4	5.6	387	213
PSf-*s*-HBTMS	5.3	21	5.10	0.96	22.2	5.31	204	137
PSf-*o*-HBTMS	5.3	70	14.6	3.29	21.3	4.44	54	133
PSf-*o*-CH_2-TMS	5.1	18	4.0	0.95	18.9	4.2	293	255
PSf-*o*-DMPS[c]	5.3	6.1	1.4	0.27	22.6	5.18	372	246
PSf-*o*-TMS[d]	5.5	29	7.1	1.3	22.3	5.3	159	99
6FPSf	5.1	12.0	3.4	0.67	17.9	5.1	373	187
6FPSf-*o*-HBTMS	5.1	105	23.9	5.63	18.6	4.25	54	114
TMPSf	5.2	21.0	5.6	1.06	19.8	5.3	252	132
TMPSf-TMS[e]	5.3	32	6.95	1.51	21.3	4.60	164	174
TMPSf-HBTMS	5.3	72	17.6	3.36	21.4	4.97	48	74

[a] Permeability coefficients measured at 35 °C and 1 atm pressure. 1 Barrer = 10^{-10} [cm^3 (STP)·cm]/(cm^2·s·cm Hg). [b] Ideal permselectivity $\alpha = (P_a)/(P_b)$. [c] Reference 26. [d] Reference 11. [e] Reference 12.

s-HBTMS. This shows a trend similar to our previous observations,[11,17,26] which is that substitution at the *ortho* ether site is more effective in increasing permeability than at the *ortho* sulfone sites. This is due to the fact that the ether linkage is more flexible and is hindered more readily by bulky substituents than the already hindered sulfone linkage. Since this effect was observed for PSf-HBTMS, the *ortho* sulfone site polymers TMPSf-*s*-HBTMS and 6FPSf-*s*-HBTMS were not prepared.

Apart from the HBTMS substituent, PSf's with other silyl substituents were compared for gas permeability data as listed in Table 6. PSf-*o*-DMPS[26] and PSf-*o*-TMS[11] were prepared previously, whereas PSf-*o*-CH_2-TMS containing an alkyl spacer was prepared for this study. Compared with other structural silyl substituents, PSf-*o*-HBTMS had significantly higher $P(CO_2)$ and $P(O_2)$ and maintained good permselectivity against N_2. Although PSf-*o*-CH_2-TMS showed increases in $P(CO_2)$ and $P(O_2)$ compared with PSf as evidenced by a slightly larger *d*-spacing of 5.1 Å compared with 5.0 Å for the PSf, it had inferior gas transport properties because the concomitant permselectivities were rather lower. This was somewhat expected because of the flexible $-CH_2-$ spacer between the polymer chain and the TMS group.

On the other hand, the silicon atom is bonded directly with the aromatic polymer chain in the PSf-*o*-DMPS polymer and the DMPS substituent contains a rigid phenyl ring on the $Si(CH_3)_2$. The overall effect of introducing this substituent was negligible since both *P* and α remained approximately the same or slightly increased. It seems likely that two opposing effects lead to this result. The steric effect of the substituent causes an increase in interchain spacing from 5.0 to 5.3 Å[26] that would be expected to show in an increase in *P*. However, the planarity of the phenyl rings on the DMPS substituent is capable of allowing more interchain packing thereby reducing the fractional free volume while maintaining permselectivity through structural rigidity. The third comparative polymer PSf-*o*-TMS had a good combination of *P* and α. PSf-*o*-HBTMS had higher permeabilities and slightly lower permselectivities than PSf-*o*-TMS, which had less space between the TMS group and the polymer chain. This is in contrast with the work of Nagai et al.[15] In this work, it was found that when a phenyl group was inserted between the TMS group and the main chain of poly[1-(trimethylsilyl)-1-propyne], interchain interactions increased resulting in a large permeability decrease.

Both 6FPSf and TMPSf have higher *P* than PSf because of the nature of the 6F group and the steric bulkiness of the tetramethyl segment. Thus, the incremental increases in *P* observed with the introduction of the HBTMS substituent were less than those for PSf. The observed increases in $P(CO_2)$ and $P(O_2)$ for 6FPSf-*o*-HBTMS were ~9-fold and ~7-fold in comparison with 6FPSf, respectively. The polymer maintained excellent $\alpha(CO_2/N_2)$, with no reduction evident. The overall result for this gas pair was a reduction in the δ distance from 0.373 to 0.054, which is close to the upper bound line. However, there was an observed decrease for $\alpha(O_2/N_2)$, with the δ distance being reduced from 0.187 to 0.114. It is clearly illustrated in Figure 4 that the decline in $\alpha(O_2/N_2)$ for 6FPSf and PSf is greater than that of the TMPSf derivative. This is in contrast to Figure 5 which shows that little or no decreases in $\alpha(CO_2/N_2)$ are observed for the polymer HBTMS derivatives of 6FPSf as well as TMPSf and PSf. 6FPSf-*o*-HBTMS was the most permeable polymer among the HBTMS polymers because of effects of both the HBTMS and the hexafluoroisopropylidene (6F) groups. Bulky HBTMS groups are responsible for forcing chain segments apart, thereby increasing permeability. From other literature studies, especially polyimides, the 6F group is known to significantly improve permeability and permselectivity by increasing chain stiffness, reducing intersegmental chain packing, and reducing interchain interactions such as charge-transfer complexes (CTCs), since CF_3 groups are electron-withdrawing and reduce CTC formation.

The highest overall increase in *P* versus α was achieved with TMPSf-HBTMS, which had a distance δ of only 0.048 for the CO_2/N_2 and 0.074 for the O_2/N_2 gas pair. Structurally, TMPSf-HBTMS contains both the tetramethylbisphenol segment as well as the HBTMS substituent, both of which increase the interchain distance. However, the HBTMS substituent is considerably larger than a methyl group such that the methyl groups may fill some space between the polymer chains and further increase chain stiffening. This may explain why TMPSf-HBTMS has both increased permeability and permselectivity for the CO_2/N_2 gas pair as shown in Figure 4. In the case of the O_2/N_2 gas pair, the TMPSf-HBTMS polymer also had the highest *P* versus α of all the derivatives, though there was a decline in permselectivity.

The HBTMS derivatives of all the polymers PSf, 6FPSf, and TMPSf all resulted in high *P* versus α for the CO_2/N_2 gas pair, all giving approximately the same distance $\delta \sim 0.05$ to the upper bound line as shown in Table 6 and Figure 4. This is remarkable in the case of PSf and TMPSf, which both had almost the same values for *P* and α. For the O_2/N_2 gas pair, the HBTMS derivatives of PSf and 6FPSf gave an almost identical *P* versus α trend, whereas the TMPSf derivative showed less reduction in permselectivity.

Conclusion

Modified PSf, 6FPSf, and TMPSf containing the novel substituent HBTMS were successfully synthesized by lithiating polymers and then treating with TMSBA. The resulting side substituent contains the bulky TMS groups separated from the polymer chain by an aromatic ring. The open structure leads to high permeability, while the substituent rigidity provides a selective diffusion environment. PSf-*o*-HBTMS, TMPSf-HBTMS, and 6FPSf-*o*-HBTMS for CO_2 and O_2 were significantly more permeable than PSf, TMPSf, and 6FPSf with little or no reduction in permselectivity (α) particularly for the CO_2/N_2 gas pair. The O_2/N_2 gas pair showed overall improvements in *P* versus α, especially for the TMPSf derivative, whose high T_g is the same as that of the starting polymer. The distances δ to the Robeson upper bound line[3] for all the HBTMS derivatives were much shorter in comparison with PSf, TMPSf, and 6FPSf, especially for the CO_2/N_2 gas pair, which remarkably all had values of $\delta \sim 0.05$. The typical *P* versus α tradeoff observed for polymers is notably absent for the CO_2/N_2 gas pair in the HBTMS derivatives. The large increases in *P* observed for gases (up to 13-fold) are ascribed to the steric restrictions of the HBTMS substituent that decrease the packing efficiency, while the retention of good permselectivity is imparted by the rigidity of the substituent.

Acknowledgment. The authors gratefully acknowledge partial financial support from the international collaboration project between the National Research Council of Canada and the Korea Institute of Science and Technology.

References and Notes

(1) Pandey, P.; Chauhan, R. S. *Prog. Polym. Sci.* **2001**, *26*, 853.
(2) Park, J. Y.; Paul, D. R. *J. Membr. Sci.* **1997**, *125*, 23.
(3) Robeson, L. M. *J. Membr. Sci.* **1991**, *62*, 165.
(4) Robeson, L. M.; Smith, C. D.; Langsam, M. *J. Membr. Sci.* **1997**, *132*, 33.
(5) Henis, J. M. S.; Tripodi, M. K. *Sep. Sci. Technol.* **1980**, *15*, 1059.
(6) Aitken, C. L.; Koros, W. J.; Paul, D. R. *Macromolecules* **1992**, *25*, 3424.
(7) Aitken, C. L.; McHattie, J. S.; Paul, D. R. *Macromolecules* **1992**, *25*, 2910.
(8) McHattie, J. S.; Koros, W. J.; Paul, D. R. *Polymer* **1992**, *33*, 1701.
(9) McHattie, J. S.; Koros, W. J.; Paul, D. R. *Polymer* **1991**, *32*, 2618.
(10) McHattie, J. S.; Koros, W. J.; Paul, D. R. *Polymer* **1991**, *32*, 840.
(11) Guiver, M. D.; Robertson, G. P.; Rowe, S.; Foley, S.; Kang, Y. S.; Park, H. C.; Won, J.; Le Thi, H. N. *J. Polym. Sci., Part A: Polym. Chem.* **2001**, *39*, 2103.
(12) Dai, Y.; Guiver, M. D.; Robertson, G. P.; Bilodeau, F.; Kang, Y.; Lee, K.; Jho, J.; Won, J. *Polymer* **2002**, *43*, 5369.
(13) Zhang, J.; Hou, X. *J. Membr. Sci.* **1994**, *97*, 275.
(14) Sisto, R.; Bonfanti, C.; Valenti, C. *J. Membr. Sci.* **1994**, *95*, 135.
(15) Nagai, K.; Masuda, T.; Nakagawa, T.; Freeman, B. D.; Pinnau, I. *Prog. Polym. Sci.* **2001**, *26*, 721.
(16) Madkour, M. *Polymer* **2000**, *41*, 7489.
(17) Lee, K. J.; Jho, J. Y.; Kang, Y. S.; Dai, Y.; Robertson, G. P.; Guiver, M. D.; Won, J. *J. Membr. Sci.* **2003**, *212*, 147.
(18) Aoki, T. *Prog. Polym. Sci.* **1999**, *24*, 951.
(19) George, S. C.; Thomas, S. *Prog. Polym. Sci.* **2001**, *26*, 985.
(20) Guiver, M. D.; ApSimon, J. W.; Kutowy, O. *J. Polym. Sci., Polym. Lett. Ed.* **1988**, *26*, 123.
(21) Guiver, M. D.; Kutowy, O.; ApSimon, J. W. *Polymer* **1989**, *30*, 1137.
(22) Guiver, M. D.; Robertson, G. P. *Macromolecules* **1995**, *28*, 294.
(23) Guiver, M. D.; Robertson, G. P.; Foley, S. *Macromolecules* **1995**, *28*, 7612.
(24) Guiver, M. D.; Zhang, H.; Robertson, G. P.; Dai, Y. *J. Polym. Sci., Part A: Polym. Chem.* **2001**, *39*, 675.
(25) Guiver, M. D.; Robertson, G. P.; Yoshikawa, M.; Tam, C. M. In *Membrane Formation and Modification*; ACS Symposium Series, No. 744; Pinnau, I., Freeman, B., Eds.; American Chemical Society: Washington, DC, 1999; Chapter 10, p 137.
(26) Kim, I.-W.; Lee, K. J.; Jho, J. Y.; Park, H. C.; Won, J.; Kang, Y. S.; Guiver, M. D.; Robertson, G. P.; Dai, Y. *Macromolecules* **2001**, *34*, 2908.
(27) Zaidi, S. M. J.; Mikhailenko, S. D.; Robertson, G. P.; Guiver, M. D.; Kaliaguine, S. *J. Membr. Sci.* **2000**, *173*, 17.
(28) Breck, D. W. In *Zeolite Molecular Sieves*; John Wiley & Sons: New York, 1974; Chapter 8, p 636.

MA0346411